J|A|C|S ARTICLES

Published on Web 09/14/2010

Experimental and Theoretical Comparison of the O K-Edge Nonresonant Inelastic X-ray Scattering and X-ray Absorption Spectra of $NaReO_4$

Joseph A. Bradley,[†,‡] Ping Yang,[||] Enrique R. Batista,*[,†] Kevin S. Boland,[†] Carol J. Burns,[†] David L. Clark,[†] Steven D. Conradson,[†] Stosh A. Kozimor,*[,†] Richard L. Martin,*[,†] Gerald T. Seidler,*[,‡] Brian L. Scott,[†] David K. Shuh,*[,§] Tolek Tyliszczak,[§] Marianne P. Wilkerson,[†] and Laura E. Wolfsberg[†]

Los Alamos National Laboratory, Los Alamos, New Mexico 87545, Department of Physics, University of Washington, Seattle, Washington 98195, Chemical Sciences Division and Advanced Light Source, Lawrence Berkeley National Laboratory, Berkeley, California 94720, and W.R. Wiley Environmental Molecular Sciences Laboratory, Pacific Northwest National Laboratory, Richland, Washington 99352

Received May 12, 2010; E-mail: stosh@lanl.gov

Abstract: Accurate X-ray absorption spectra (XAS) of first row atoms, e.g., O, are notoriously difficult to obtain due to the extreme sensitivity of the measurement to surface contamination, self-absorption, and saturation affects. Herein, we describe a comprehensive approach for determining reliable O K-edge XAS data for ReO_4^{1-} and provide methodology for obtaining trustworthy and quantitative data on nonconducting molecular systems, even in the presence of surface contamination. This involves comparing spectra measured by nonresonant inelastic X-ray scattering (NRIXS), a bulk-sensitive technique that is not prone to X-ray self-absorption and provides exact peak intensities, with XAS spectra obtained by three different detection modes, namely total electron yield (TEY), fluorescence yield (FY), and scanning transmission X-ray microscopy (STXM). For ReO_4^{1-}, TEY measurements were heavily influenced by surface contamination, while the FY and STXM data agree well with the bulk NRIXS analysis. These spectra all showed two intense pre-edge features indicative of the covalent interaction between the Re 5d and O 2p orbitals. Density functional theory calculations were used to assign these two peaks as O 1s excitations to the e and t_2 molecular orbitals that result from Re 5d and O 2p covalent mixing in T_d symmetry. Electronic structure calculations were used to determine the amount of O 2p character (%) in these molecular orbitals. Time dependent-density functional theory (TD-DFT) was also used to calculate the energies and intensities of the pre-edge transitions. Overall, under these experimental conditions, this analysis suggests that NRIXS, STXM, and FY operate cooperatively, providing a sound basis for validation of bulk-like excitation spectra and, in combination with electronic structure calculations, suggest that $NaReO_4$ may serve as a well-defined O K-edge energy and intensity standard for future O K-edge XAS studies.

Introduction

Several recent studies have highlighted the growing popularity and utility of using ligand K-edge X-ray absorption spectroscopy (XAS) as a direct probe of covalent mixing in metal−ligand bonding.[1−21] Seminal work by Solomon, Hedman, Hodgson, and their students has established that the intensities of bound state transitions observed in the pre-edge region of ligand K-edge XAS spectra are directly related to the amount of orbital mixing in a given metal−ligand bond.[6] A prominent and popular suite of elements for study by ligand K-edge XAS spectroscopy has been the duo of Cl and S, which have been widely examined for inorganic and bioinorganic molecules of the transition elements and recently extended to actinide systems.[1−21]

In light of such success, it seems that developing the use of synchrotron-generated radiation to quantify covalency for ligands other than Cl and S would have wide impact. This is especially true for light atoms (B, C, N, O, and F), given that these elements form the basis of many common ligands and

[†] Los Alamos National Laboratory.
[‡] University of Washington.
[§] Lawrence Berkeley National Laboratory.
[||] Pacific Northwest National Laboratory.

(1) Hedman, B.; Hodgson, K. O.; Solomon, E. I. *J. Am. Chem. Soc.* **1990**, *112*, 1643.
(2) Shadle, S. E.; Hedman, B.; Hodgson, K. O.; Solomon, E. I. *Inorg. Chem.* **1994**, *33*, 4235.
(3) Shadle, S. E.; Hedman, B.; Hodgson, K. O.; Solomon, E. I. *J. Am. Chem. Soc.* **1995**, *117*, 2259.
(4) Glaser, T.; Hedman, B.; Hodgson, K. O.; Solomon, E. I. *Acc. Chem. Res.* **2000**, *33*, 859.
(5) Szilagyi, R. K.; Bryngelson, P. A.; Maroney, M. J.; Hedman, B.; Hodgson, K. O.; Solomon, E. I. *J. Am. Chem. Soc.* **2004**, *126*, 3018.
(6) Solomon, E. I.; Hedman, B.; Hodgson, K. O.; Dey, A.; Szilagyi, R. K. *Coord. Chem. Rev.* **2005**, *249*, 97.
(7) DeBeer George, S.; Brant, P.; Solomon, E. I. *J. Am. Chem. Soc.* **2005**, *127*, 667.
(8) DeBeer George, S.; Huang, K.-W.; Waymouth, R. M.; Solomon, E. I. *Inorg. Chem.* **2006**, *45*, 4468.

10.1021/ja1040978

have a propensity to form multiple bonds with unusual stability, largely attributed to covalent metal−ligand bonding.[22−32] In addition, variation in metal identity, oxidation state, ancillary ligand, and coordination number dramatically affect the metal−ligand multiple bond stability, such that highly reactive oxo,[22−24,27,30] imido,[23,25,29] alkylidene, and alkylidyne[23,28,31,32] ligands have been identified that play central roles for key bond forming and breaking reactions in bioinorganic chemistry and catalysis. However, quantitative light atom ligand K-edge XAS analyses on these types of compounds have historically been difficult given the numerous obstacles associated with the experiment. These difficulties largely stem from the low energy associated with light atom K-edge excitations (180−700 eV), which renders these measurements as extremely sensitive to surface contamination, self-absorption, and saturation effects. Such issues become magnified when nonconducting molecular systems are analyzed and when surface contamination cannot be removed by standard techniques, i.e., cleaving crystals under vacuum. Unfortunately, if any such complications arise, uncontrolled systematic errors result that prohibit quantitative experimental determination of orbital mixing.

Recent advances in instrumentation associated with new beamlines at synchrotron user facilities have allowed us to characterize the magnitude of these problems and obtain reproducible O K-edge XAS spectra that can be used to directly probe covalency. Specifically, we explored the nonresonant inelastic X-ray scattering (NRIXS) technique in comparison to X-ray absorption spectroscopy (XAS). In order to understand the origin of this comparison, consider that in conventional XAS the X-ray absorption coefficient, μ, can be described by

$$\mu(\hbar,\omega_i) = |\langle f|\boldsymbol{\varepsilon}\cdot\mathbf{r}|0\rangle|^2\delta(E_f - E_0 - \hbar\omega_i) \quad (1)$$

where ω_i is the energy of the incoming photon, $\boldsymbol{\varepsilon}$ is its polarization, and the labels 0 and f refer to the initial and final states, respectively. In contrast, the NRIXS double differential cross section is proportional to the dynamic structure factor

$$S(q,\omega) = |\langle f|e^{iq\cdot r}|0\rangle|^2\delta(E_f - E_0 - \hbar\omega) \quad (2)$$

where ω is the energy loss of the incoming photon and q is the momentum transfer.[33] Although eq 2 seems quite different than eq 1, when the momentum transfer is small, i.e., $q \ll 1/r_0$ (where r_0 characterizes the radius of the initial state) the $e^{iq\cdot r}$ operator simplifies to $\mathbf{q}\cdot\mathbf{r}$,[33]

$$S(q,\omega) \approx |\langle f|\mathbf{q}\cdot\mathbf{r}|0\rangle|^2\delta(E_f - E_0 - \hbar\omega) \quad (3)$$

For nonordered polycrystalline samples, as in the current case, the directional dependence of the NRIXS momentum transfer vector, $\mathbf{q}$, and the XAS polarization vector, ε, average away. As a consequence of these formal similarities, the XAS and low-q NRIXS measurements provide equivalent information if they probe comparable populations of atoms in a given sample.[34]

Despite the similarities between low-q NRIXS and XAS, the core electronic excitation mechanisms are quite different, Scheme 1. For XAS, O 1s electronic excitations occur when

Scheme 1

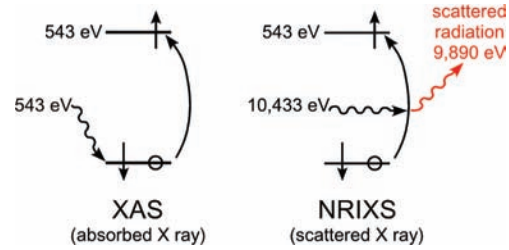

an X-ray is absorbed by the analyte, and the energy of the incident radiation equals the energy of the electronic excitation. In contrast, for NRIXS the energy for the analogous electronic excitation comes from the energy *lost* by a high energy hard X-ray photon (∼6−10 keV) during an inelastic scattering event.[34] Because of the high energy associated with the incident photon, NRIXS light-atom K-edge measurements are immune to the surface contamination and self-absorption affects that can be so problematic in traditional light-atom XAS.[33−36]

Contributed here is an analysis of the O K-edge spectrum of the ReO_4^{1-} ion obtained by NRIXS and a full battery of XAS detection methods: total electron yield (TEY),[37] fluorescence yield (FY),[37] and scanning transmission X-ray microscopy (STXM).[38−42] Conducting measurements in all four modes

(9) Delgado-Jaime, M. U.; Conrad, J. C.; Fogg, D. E.; Kennepohl, P. *Inorg. Chim. Acta* **2006**, *359*, 3042.
(10) Ray, K.; DeBeer George, S.; Solomon, E. I.; Wieghardt, K.; Neese, F. *Chem.—Eur. J.* **2007**, *13*, 2783.
(11) Dey, A.; Jeffrey, S. P.; Darensbourg, M.; Hodgson, K. O.; Hedman, B.; Solomon, E. I. *Inorg. Chem.* **2007**, *46*, 4989.
(12) Doonan, C. J.; Rubie, N. D.; Peariso, K.; Harris, H. H.; Knottenbelt, S. Z.; George, G. N.; Young, C. G.; Kirk, M. L. *J. Am. Chem. Soc.* **2008**, *130*, 55.
(13) Sarangi, R.; York, J. T.; Helton, M. E.; Fujisawa, K.; Karlin, K. D.; Tolman, W. B.; Hodgson, K. O.; Hedman, B.; Solomon, E. I. *J. Am. Chem. Soc.* **2008**, *130*, 676.
(14) Shearer, J.; Dehestani, A.; Abanda, F. *Inorg. Chem.* **2008**, *47*, 2649.
(15) Kozimor, S. A.; Yang, P.; Batista, E. R.; Boland, K. S.; Burns, C. J.; Christensen, C. N.; Clark, D. L.; Conradson, S. D.; Hay, P. J.; Lezama, J. S.; Martin, R. L.; Schwarz, D. E.; Wilkerson, M. P.; Wolfsberg, L. E. *Inorg. Chem.* **2008**, *47*, 5365.
(16) Harkins, S. B.; Mankad, N. P.; Miller, A. J. M.; Szilagyi, R. K.; Peters, J. C. *J. Am. Chem. Soc.* **2008**, *130*, 3478.
(17) Adhikari, D.; Mossin, S.; Basuli, F.; Huffman, J. C.; Szilagyi, R. K.; Meyer, K.; Mindiola, D. J. *J. Am. Chem. Soc.* **2008**, *130*, 3676.
(18) Mankad, N. P.; Antholine, W. E.; Szilagyi, R. K.; Peters, J. C. *J. Am. Chem. Soc.* **2009**, *131*, 3878.
(19) Dey, A.; Jiang, Y.; Ortiz de Montellano, P.; Hodgson, K. O.; Hedman, B.; Solomon, E. I. *J. Am. Chem. Soc.* **2009**, *131*, 7869.
(20) Kozimor, S. A.; Yang, P.; Batista, E. R.; Boland, K. S.; Burns, C. J.; Clark, D. L.; Conradson, S. D.; Martin, R. L.; Wilkerson, M. P.; Wolfsberg, L. E. *J. Am. Chem. Soc.* **2009**, *131*, 12125.
(21) Sriskandakumar, T.; Petzold, H.; Bruijnincx, P. C. A.; Habtemariam, A.; Sadler, P. J.; Kennepohl, P. *J. Am. Chem. Soc.* **2009**, *131*, 13355.
(22) Holm, R. H. *Chem. Rev.* **1987**, *87*, 1401.
(23) Nugent, W. A.; Mayer, J. M. *Metal-Ligand Multiple Bonds*; Wiley-Interscience: New York, 1988.
(24) Jorgensen, K. A.; Shioett, B. *Chem. Rev.* **1990**, *90*, 1483.
(25) Wigley, D. E. *Prog. Inorg. Chem.* **1994**, *42*, 239.
(26) Parkin, G. *Prog. Inorg. Chem.* **1998**, *47*, 1.
(27) Mayer, J. M. *Acc. Chem. Res.* **1998**, *31*, 441.
(28) Schrock, R. R. *Chem. Rev.* **2002**, *102*, 145.
(29) Hazari, N.; Mountford, P. *Acc. Chem. Res.* **2005**, *38*, 839.
(30) Bakac, A. *Coord. Chem. Rev.* **2006**, *250*, 2046.
(31) Mindiola, D. J. *Acc. Chem. Res.* **2006**, *39*, 813.
(32) Vougioukalakis, G. C.; Grubbs, R. H. *Chem. Rev.* **2010**, *110*, 1746.
(33) Soininen, J. A.; Ankudinov, A. L.; Rehr, J. J. *Phys. Rev. B* **2005**, *72*, 045136.
(34) Schuelke *Electron Dynamics by Inelastic Scattering*; Oxford University Press: New York, 2007.
(35) Bergmann, U.; Glatzel, P.; Cramer, S. P. *Microchem. J.* **2002**, *71*, 221.
(36) Ruocco, G.; Sette, F.; Bergmann, U.; Krish, M.; Masciovecchio, C.; Mazzacurati, V.; Signorelli, G.; Verbeni, R. *Nature* **1996**, *379*, 521.
(37) Stöhr, J. *NEXAFS Spectroscopy*; Springer Series in Surface Sciences: Berlin, 1992.
(38) Thompson, A.; Attwood, D.; Gullikson, E.; Howells, M.; Kim, K.-J.; Kirz, J.; Kortright, J.; Lindau, I.; Pianetta, P.; Robinson, A.; Scofield, J.; Underwood, J.; Vaughan, D.; Williams, G.; Winich, G. *X-ray Data Booklet*; Lawrence Berkley National Laboratory: Berkeley, CA, 2001.

provides a comprehensive evaluation of the sampled material and allows unambiguous experimental determination of accurate, bulk-sensitive results. In addition, we find that hybrid density functional theory (DFT) calculations can be used to guide the interpretation of the $NaReO_4$ spectra. Overall, these results show that NRIXS and XAS measurements, made in conjunction with DFT calculations, provide a platform for further development of light atom ligand K-edge spectroscopy as a direct probe for orbital mixing.

Experimental Section

General Considerations. The compounds and samples were prepared and manipulated under helium, argon, or nitrogen with rigorous exclusion of air and moisture using standard Schlenk, glovebox, and glovebag techniques. Toluene was distilled over sodium and benzophenone and degassed by three freeze−pump−thaw cycles. Polystyrene (PolySciences Inc.) was acquired as 3.0 Micron Dry Form and dried under vacuum (10^{-3} Torr) for 24 h. Both $NaReO_4$ (Aldrich), which was crystallized from H_2O, and carbon (Vulcan XC-72; Cabot Corp) were heated (150 °C) under vacuum (10^{-3} Torr) for 24 h prior to use. The structure of $NaReO_4$ was confirmed by X-ray crystallography to contain $(ReO_4)^{1-}$ units that are of tetrahedral symmetry, with 1.722(5) Å average Re−O distances and 109.62(21)° average O−Re−O angles, which is consistent with previous reports.[43,44]

Oxygen K-Edge NRIXS Measurements. The NRIXS samples were prepared in a helium-filled glovebox by finely grinding the $NaReO_4$ (0.070 g) with polystyrene beads (0.030 g) to obtain a homogeneous mixture that contained, by mass, 70% analyte. Toluene (400 μL) was added, and the mixture was stirred with a glass stir rod until the polystyrene dissolved. The resulting solution was transferred to a 4−10 mm slot in an aluminum sample plate, which had been secured to a Teflon block. After 48 h the toluene evaporated, leaving a robust film fixed within the sample block that was cut free from the slot using a razor blade.

All NRIXS measurements were taken using the lower energy resolution inelastic X-ray scattering (LERIX) user facility at the PNC/XOR 20-ID beamline of the Advanced Photon Source.[45] This undulator beamline uses a double-crystal Si (111) monochromator and has a typical incident photon flux of $\sim 10^{12}$/s. The net energy resolution (fwhm) of the monochromator and the LERIX analyzer crystals is 1.3 eV, as determined from the width of the elastic scattering line. Initial NRIXS data extraction and processing followed methods reported previously.[45,46] The dipole approximation to the NRIXS cross section (eq 2) was verified by the independence of the oxygen K-edge shape over the range of q reported. As a consequence, the reported NRIXS spectra are obtained by combining the counts from six different detectors spanning from $q = 3.3$ to 4.8 a.u. The typical measurement time per data point is 80 s, which yields ~5000 counts in the q-integrated edge step above ~60 000 counts from background due to the valence Compton scattering. Although the polystyrene matrix darkened in color during the measurement, the NRIXS data for $NaReO_4$ spectra showed no sign of radiation damage and was reproduced on different sections of the polystyrene film.

Oxygen K-Edge TEY and FY Measurements. Samples were prepared in a helium filled glovebox by initially degassing a solution that contained polystyrene (2.002 g) and toluene (6.564 g) by freeze−pump−thaw cycles (3×). An aliquot of this solution (0.171 g) was added to a mixture of $NaReO_4$ (0.070 g) and carbon (0.010 g), which had been finely ground with a mortar and pestle. This mixture was stirred with a glass rod and transferred into a 5 × 11 × 4 mm well that had been bored into an aluminum block. The toluene was allowed to evaporate for 48 h under a helium atmosphere in a glovebox, which left a robust film fixed within the sample block that contained (by mass) approximately 58% $NaReO_4$. The block was transferred with rigorous exclusion of air and moisture to a sputter-coating system and a 10 to 15 Å layer of carbon was deposited onto the surface of the sample.

Room temperature O K-edge XAS data were recorded at the Stanford Synchrotron Radiation Lightsource (SSRL) and analyzed at VUV beamline 8−2, utilizing bending magnet radiation and a spherical grating monochromator, under ring conditions of 3.0 GeV and 85−100 mA in high magnetic field mode of 0.9 T. A chamber similar to that previously described[47] was used, with the exception that a 1200 Å carbon window was used to isolate the chamber from the beam pipe. The incident radiation was monitored using a Au grid with 80% transmission. Both the total electron yield (TEY, total current leaving the sample) and sample excitation fluorescence were simultaneously collected under vacuum (10^{-7} Torr) as a function of the incident beam energy. The fluorescence was measured using an identically configured pair of International Radiation Detector XUV100 type photodiodes coated with 1000 Å of aluminum. The photodiodes were closely spaced so that a 1−2 mm wide beam passed between them. The diodes were mounted facing the sample at normal incidence to the oncoming beam and in close proximity to the sample (5−10 mm). The TEY and FY data for $NaReO_4$ spectra showed no sign of radiation damage and the spectra were reproduced for multiple samples during three different synchrotron experiments.

Oxygen K-Edge STXM Measurements. In an argon-filled glovebox, $NaReO_4$ (30 mg) was ground in a mortar and pestle, and the particles were transferred to a Si_3N_4 window (100 nm). A second window was placed over the sample, essentially sandwiching the $NaReO_4$ particles, and the windows were sealed together using epoxy.

Single-energy images and oxygen K-edge XAS spectra were acquired using the STXM instrument at the Advanced Light Source Molecular Environmental Science beamline 11.0.2, which is operated in topoff mode at 500 mA, in a ~0.5 atm He filled chamber. For these measurements, the X-ray beam was focused with a zone plate onto the sample, and the transmitted light was detected. The spot size and spectral resolution were determined from characteristics of the 35 nm zone plate. Images at a single energy were obtained by raster-scanning the sample and collecting transmitted monochromatic light as a function of sample position. Spectra at each image pixel or particular regions of interest on the sample image were extracted from the "stack", which is a collection of images recorded at multiple, closely spaced photon energies across the absorption edge.[48] This enabled spatial mapping of local chemical bonding information. Dwell times used to acquire an image at a single photon energy were ~1 ms per pixel. To quantify the absorbance signal, the measured transmitted intensity (I) was converted to optical density using Beer−Lambert's law:[49] $OD = \ln(I/I_0) = \mu\rho d$, where I_0 is the incident photon flux intensity, d is the sample thickness, and μ and ρ are the mass absorption coefficients and density of the sample material, respectively.

(39) Bluhm, H.; et al. *J. Electron Spectrosc. Relat. Phenom.* **2006**, *150*, 86.
(40) Warwick, T.; et al. *Rev. Sci. Instrum.* **1998**, *69*, 2964.
(41) Minasian, S. G.; Krinsky, J. L.; Rinehart, J. D.; Copping, R.; Tyliszczak, T.; Janousch, M.; Shuh, D. K.; Arnold, J. *J. Am. Chem. Soc.* **2009**, *38*, 13767.
(42) Nilsson, H. J.; Tyliszczak, T.; Wilson, R. E.; Werme, L.; Shuh, D. K. *J. Anal. Bioanal. Chem.* **2005**, *383*, 41.
(43) Atzesdorfer, A.; Range, K. J. *Z. Naturfosch., B: Anorg. Chem.* **1995**, *50*, 1417.
(44) Beintema, J. *Strukturbericht* **1937**, *3*, 421.
(45) Fister, T. T.; Seidler, G. T.; Wharton, L.; Battle, A. R.; Ellis, T. B.; Cross, J. O.; Macrander, A. T.; Elam, W. T.; Tyson, T. A.; Qian, Q. *Rev. Sci. Instrum.* **2006**, *77*, 063901.
(46) Fister, T. T.; Seidler, G. T.; Hamner, C.; Cross, J. O.; Soininen, J. A.; Rehr, J. J. *Phys. Rev. B* **2006**, *74*, 214177.
(47) Shadle, S. E. Ph.D. Thesis; Stanford University: Stanford, CA, 1994.
(48) Hitchcock, A. P. *aXis Version 17-Sep-08*; McMaster University: Hamilton, Ontario, Canada.
(49) Tivanski, A. V.; Hopkins, R. J.; Tyliszczak, T.; Gilles, M. K. *J. Phys. Chem. A* **2007**, *111*, 5448.

Incident beam intensity was measured through the sample-free region of the Si_3N_4 windows. Particle spectra were then obtained by averaging over the particles deposited on the substrate.[48] Regions of particles with an absorption of >1.5 OD were omitted to ensure the spectra were in the linear regime of the Beer−Lambert law. The energy resolution (fwhm) was determined to be 0.08 eV. During the STXM experiment, $NaReO_4$ particles showed no sign of radiation damage and the spectrum was reproduced for multiple particles.

Data Analysis. Data manipulation and analyses were performed with slight modifications to those described by Solomon and coworkers.[6] In typical data analysis, a first-order polynomial was fit to the pre-edge region (<520 eV) and then subtracted from the experimental data to eliminate the background of the spectrum. The data were then normalized by fitting a first-order polynomial to the postedge region of the spectrum (>545 eV) and by setting the magnitude of this second line (the edge step) at 542.0 eV to an intensity of 1.0. The TEY, FY, and STXM data were calibrated in energy by shifting them to match the first pre-edge feature of the NRIXS spectrum at 531.40 eV. Curve-fitting analyses were conducted with mathematical expressions employed in EDG_FIT,[50] which for convenience were transported to the IGOR 6.04 platform, and fits were performed over several energy ranges. The first and second derivatives of each spectrum were used as guides to determine the number and positions of the spectral features for the curve-fitting analyses. For the pre-edge, white line, and postedge features, Gaussian functions were used, and for the step function, a 1:1 ratio of arctan and error function contributions were employed.[6]

Electronic Structure Calculations. Electronic structure calculations were conducted on ReO_4^{1-} using B3LYP hybrid density functional theory (DFT)[51] in the Gaussian 03 code.[52] The Stuttgart 97 relativistic effective core potential (RECP) and associated basis sets (minus the most diffuse function) were used for Re, whereas for O we used the double-ζ basis set. These functionals and basis sets have been extensively tested for organometallic and inorganic systems and have been shown to give good agreement with experimental data.[15,20,53−58] The populations of the O 2p orbitals of each compound were then obtained by Mulliken population analysis of each particular molecular orbital. Because this combination of tools predicts a relatively small splitting between the unoccupied Re 5d and 6d orbitals (vide infra), some tests were run to verify this prediction: [1] A further diffused d basis function was added with an exponent of 0.013, following an even-tempered progression from the already existent Gaussians; [2] a full shell of f functions was added to identify the Re 5f orbitals; [3] to test for the presence of the environment, a polarizable continuum was added around the ReO_4^{1-} complex with a dielectric constant of 78; and [4] test 3 was run with the extra diffused d function indicated in test 1. All of these calculations give very similar results, and these are discussed in the Supporting Information.

Simulated O K-Edge Spectra. The O K-edge X-ray absorption spectra of T_d ReO_4^{1-} were simulated using time dependent-density functional theory (TD-DFT). The TD-DFT output was analyzed in a natural transition orbital picture[59,60] to extract the relative participation of the various atomic components and angular momenta of the final state. These calculations were conducted as previously described[20] and involve evaluating core electron excitations by exploiting the small amount of mixing of the core orbitals with the high-lying unoccupied virtual orbitals. Specifically, this analysis involves a linear response calculation for extracting the probability amplitudes from the transition densities and dipole moments between the calculated excited states and the ground states. The excitations originating from all of the intermediate states between the O 1s and the HOMO were excluded so that only excitations from the core levels to virtual molecular orbitals could be analyzed. This allows the virtual orbitals to mix and reflect the presence of the core hole in oxygen. Relaxations for the other occupied orbitals associated with the core hole are not included. Although excluding relaxations in the occupied orbitals associated with the core hole results in large errors associated with absolute calculated transition energies, this computation technique addresses the first order changes in virtual orbitals accompanying the core hole excitation. Previously these calculations have provided very good agreement with experimental measurements made on transition metal compounds.[15,20] A constant shift of 13.7 eV was applied to the calculated O K-edge spectrum to account for the omission of the atomic relaxation associated with the core excitation, relativistic stabilization, and errors associated with the functional for the closed shell.[61]

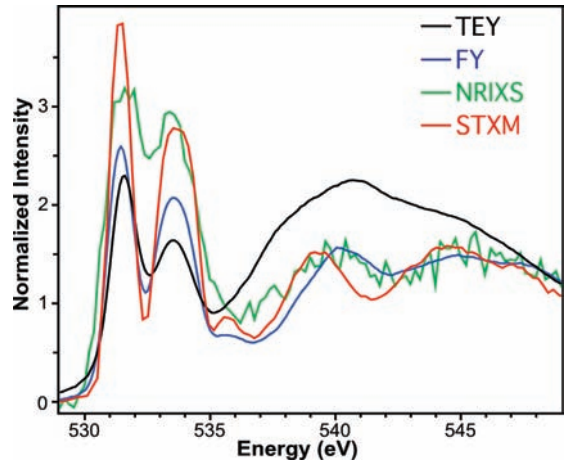

Figure 1. O K-edge spectra for polystyrene encapsulated samples of $NaReO_4$ obtained by total electron yield (TEY; black), fluorescence yield (FY; blue), and nonresonant inelastic X-ray scattering (NRIXS; green) are compared with a scanning transmission X-ray microscopy (STXM; red) measurement made on a $NaReO_4$ single particle.

Results and Discussion

Oxygen K-Edge Measurements. The O K-edge NRIXS[33−36] spectrum for $NaReO_4$ is compared to XAS data obtained by total electron yield (TEY),[37] fluorescence yield (FY),[37] and scanning transmission X-ray microscopy (STXM)[38,39] in Figure 1. Although the profiles and relative energies of the features in all four spectra are qualitatively similar, there are significant differences between each data set. To understand these varia-

(50) George, G. N., *EDG_FIT, Stanford Synchrotron Radiation Laboratory, Stanford Linear Accelerator Center*; Stanford University: Stanford, CA.
(51) Becke, A. D. *J. Chem. Phys.* **1993**, *98*, 5648.
(52) Frisch, M. J.; et al. *Gaussian 03*; Gaussian Inc.: Wallingford, CT, 2004.
(53) Küchle, W.; Dolg, M.; Stoll, H.; Preuss, H. *J. Chem. Phys.* **1994**, *100*, 7535.
(54) Clark, A. E.; Martin, R. L.; Hay, P. J.; Green, J. C.; Jantunen, K. C.; Kiplinger, J. L. *J. Phys. Chem. A* **2005**, *109*, 5481.
(55) Bi, S; Lin, Z; Jordan, R. F. *Organometallics* **2004**, *23*, 4882.
(56) Hay, P. J. *Organometallics* **2007**, *26*, 4424.
(57) Karttunen, V. A.; Linnolahti, M.; Pakkanen, T. A.; Maaranen, J.; Pitkänen, P. *Theo. Chem. Acc.* **2007**, *118*, 899.
(58) Graves, C. R.; Yang, P.; Kozimor, S. A.; Vaughn, A. E.; Clark, D. L.; Conradson, S. D.; Schelter, E. J.; Scott, B. L.; Thompson, J. D.; Hay, P. J.; Morris, D. E.; Kiplinger, J. L. *J. Am. Chem. Soc.* **2008**, *130*, 5272.
(59) Martin, R. L. *J. Chem. Phys.* **2003**, *118*, 4775.
(60) Batista, E. R. Martin, R. L. Natural transition orbitals. In *Encyclopedia of Computational Chemistry*; Schleyer, P. V. R., Allinger, N. L., Clark, T., Gasteiger, J., Kollman, P. A., Schaefer, H. F., III, Schreiner, P. R., Eds.; Oxford: Chichester, U.K., 2004.
(61) Martin, R. L.; Shirley, D. A., Many-electron theory of Photoemission. In *Electron Spectroscopy, Theory, Techniques and Applications*; Academic Press: New York, 1977; Vol. 1, p 75.

Table 1. Comparison of the Experimentally Determined and Calculated Pre-Edge Peak Energies (eV), Full-Width Half-Height (FWHM; eV), Peak Height (PH; Normalized Intensity), and Peak Intensity (Int)[b] for $NaReO_4$[a]

	peak 1				peak 2				peak 3			
technique	energy	fwhm	PH	Int	energy	fwhm	PH	Int	energy	fwhm	PH	Int
TD-DFT (calc)	531.4				533.7				535.7			
FY	531.4	1.20	2.54	3.25	533.6	1.98	2.11	4.45	535.9	1.53	0.42	0.68
STXM	531.4	0.97	4.03	4.16	533.7	1.80	2.97	5.69	535.9	1.13	0.62	0.75
NRIXS	531.4	1.60	2.92	4.98	533.5	2.30	2.84	6.96	535.9[c]	1.70[c]	0.41[c]	0.74[c]

[a] The fluorescence yield (FY) and scanning transmission X-ray microscopy (STXM) data obtained via X-ray absorption spectroscopy (XAS) is compared with the nonresonant inelastic X-ray scattering (NRIXS) data and the time dependent-density functional theory (TD-DFT) calculations. [b] Peak intensities (Int) were determined by multiplying the fwhm by the PH by 1.065, which is a constant associated with the curve fitting data analysis routine. [c] The NRIXS parameters associated with peak 3 were constrained based on the STXM data.

tions, it is instructive to begin by comparing the TEY and FY measurements. Both spectra exhibit two low energy pre-edge features at approximately 531.4 and 533.6 eV, Table 1, which have comparable peak energies and peak splittings. However, the FY spectrum contains an additional pre-edge feature at 535.87 eV. Although this feature might also be present in the TEY measurement, it could not be resolved from the rising edge, whose line shape is appreciably different from the FY data. The strong differences between TEY and FY measurements in the postedge region (>536 eV) unequivocally show that the two modes are probing oxygen in different chemical environments. These differences could result from some degree of surface contamination that influences the surface-sensitive TEY measurement or from complications in the FY measurement, i.e., self-absorption. Regardless of the cause, without corroboration of one mode over the other, it is impossible to draw conclusions from the FY and TEY data alone.

To provide arbitration, the O K-edge spectrum of $NaReO_4$ was measured with nonresonant inelastic X-ray scattering (NRIXS). This allows low-energy transitions to be probed using high-energy X-rays (~10 keV), and consequently provides O K-edge spectra for the bulk phase of the material. In this case, it was determined that the FY spectrum in Figure 1 is representative of the bulk sample since the pre- and postedge features agree well with the NRIXS measurement, although as expected the peak intensities are affected by the FY self-absorption. In contrast the pre- and postedge regions of the TEY spectrum, which like NRIXS are not affected by self-absorption, are unique, suggesting that the TEY data is not representative of the bulk sample. Although correct TEY spectra can likely be obtained on $NaReO_4$ using different methods for sample preparation, these results demonstrate the difficulty in obtaining correct TEY spectra when the analyte is encapsulated in polystyrene films. Although NRIXS often finds application for probing low-energy excitations for samples that are incompatible with traditional XAS measurements,[62−64] these results show the value in comparing bulk and surface-sensitive techniques, when possible.

Although NRIXS does provide a method for measuring low energy O K-edge excitations on bulk material, it is limited by a small interaction cross section that can lead to long acquisition times and high statistical noise in comparison to more typical XAS measurements. In addition, the ~1.3 eV NRIXS energy resolution was substantially broader than that of the XAS measurements, e.g. the FY resolution is 0.7 eV. This becomes increasingly important when trying to resolve subtleties in the pre-edge regions of the FY and NRIXS spectra of $NaReO_4$. For example, the two data sets agree strongly on the location of the two main pre-edge features at approximately 531.4 and 533.5 eV, see Table 1. However, it is not possible to determine if the third weak feature (535.9 eV) in the FY data is also present in the NRIXS spectrum.

Initially in the FY data, it seemed possible that the third feature at 535.9 eV was attributable to the K-edge of the Na^{1+} cation excited by the second energy harmonic, which is not rejected by the spherical grating monochromator. However, insertion of a 2500 Å cobalt filter, which preferentially attenuates flux at energies above 778 eV, did not remove the feature. In an attempt to confirm that this peak was indeed a component of the O K-edge spectrum of ReO_4^{1-}, XAS spectra were recorded using scanning transmission X-ray microscopy (STXM). Since the FY and STXM spectra both contain the weak feature at 535.9 eV, and because the ALS-MES undulator beamline 11.0.2 has extremely low contributions from second-order radiation,[38,39,49] we conclude that in addition to the two major pre-edge features the third weak feature is a legitimate part of the bulk $NaReO_4$ O K-edge spectrum.

Curve Fitting Analysis. The FY, STXM, and NRIXS spectra were modeled using symmetrically constrained Gaussian line shapes and a step function with a 1:1 ratio of arctan and error function contributions, Figure 2 and Table 1. These constraints provided models with good correlation coefficients, residual data that only slightly deviated from zero, and symmetric residual peaks that were similar in shape to the corresponding Gaussian functions, see the Supporting Information.[20] Initially, the NRIXS spectrum was modeled using only two pre-edge features. However, since the pre-edge region of the FY and STXM fits required three features at approximately 531.4, 533.6, and 535.9 eV, a third NRIXS pre-edge feature was added, whose peak position and height were constrained based on the STXM model, while accounting for the lower energy resolution in the NRIXS measurement. Including this third feature in the NRIXS fits did not appreciably affect the intensities and energies of the first two features, because the primary source of uncertainty in these values is associated with the line shape at the onset of the edge (>535 eV) which is included in the NRIXS uncertainty. Thus, although the NRIXS data allows definitive conclusions to be made regarding the model parameters associated with the first two pre-edge features, the lower energy resolution and higher statistical noise forbids using this NRIXS data alone to quantify the peak position and intensity of the third high energy pre-edge feature.

To investigate if $NaReO_4$ has potential to serve as a well-defined intensity standard for subsequent covalency studies on

(62) Balasubramanian, M.; Johnson, C. S.; Cross, J. O.; Seidler, G. T.; Fister, T. T.; Stern, E. A.; Hamner, C.; Mariager, S. O. *Appl. Phys. Lett.* **2007**, *91*, 031904.
(63) Conrad, H.; Lehmkühler, F; Sternemann, C.; Feroughi, O.; Simonelli, L.; Huotari, S.; Tolan, M. *Rev. Sci. Instrum.* **2009**, *80*, 026103.
(64) Rueff, J. P.; Shukla, A. *Rev. Mod. Phys.* **2010**, *82*, 847.

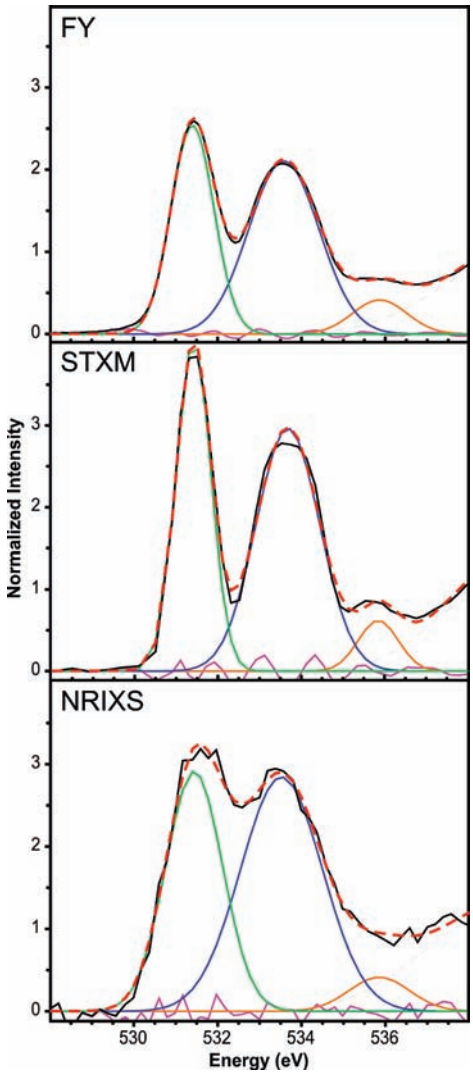

Figure 2. O K-edge X-ray absorption spectra obtained by fluorescence yield (FY; top), scanning transmission X-ray microscopy (STXM; middle), and nonresonant inelastic X-ray scattering (NRIXS; bottom). The data (black), curve fits (red dashes), residual data (pink), and pre-edge Gaussian peaks used to generate the fit (green, blue, and orange) are shown.

M−O bonding, the pre-edge intensities were quantified using the curve-fitting analysis. For this purpose, the FY measurement is not as useful since the pre-edge intensities, Table 1, are likely affected by self-absorption effects that result from high analyte concentration and large particle size compared to characteristic X-ray penetration lengths ($\sim$1 μm) at these energies. However, correct pre-edge peak intensities of 4.98 and 6.96 were obtained using NRIXS, whose O 1s electron excitation mechanism is unaffected by saturation and self-absorption effects. These values were confirmed using the STXM measurement, which in principle provides quantitative pre-edge intensities, so long as the absorption of the analyzed particle has an optical density <1.5 and is in the linear regime of the Beer−Lambert law.[49] Such was the situation in this experiment, and the STXM pre-edge peak intensities of 4.16, 5.69, and 0.75 are indistinguishable from the NRIXS data within 2σ, given that varying the fitting parameters of the higher energy features in each spectra provided estimated 5% and 10% uncertainties associated with the STXM and NRIXS measurements, respectively.

Ground State DFT Calculations. To assign the transitions responsible for the pre-edge features in the $NaReO_4$ O K-edge spectrum, group theory analysis and DFT calculations were conducted. For the tetrahedral ReO_4^{1-} ion, group theory reminds us that the O 2p lone pair orbitals can be characterized as having either σ- or π-symmetry with respect to the Re−O bond. With this designation, the O 2p σ-orbitals span $a_1 + t_2$ symmetries and the O 2p π-orbitals span $t_1 + t_2 + e$ symmetries. The rhenium ion can form Re−O σ-bonds of $a_1 + t_2$ symmetries and Re−O π-bonds of $t_2 + e$ symmetries, leaving the non-interacting t_1 combination of O 2p orbitals as nonbonding oxygen lone pairs, Figure 3. These Re−O interactions give the well-known tetrahedral e and t_2 metal based orbitals that are Re−O antibonding.[65−76] This well-established molecular orbital picture forms the basis for interpretation of the O K-edge XAS spectrum of T_d-ReO_4^{1-}, and predicts two pre-edge features stemming from excitation of O 1s electrons (a_1 and t_2) to unoccupied Re e and t_2 MOs that contain O 2p antibonding character due to Re−O orbital mixing, Figure 3. This interpretation is heavily supported by the extensive Cl K-edge XAS work previously conducted on transition metal tetrahalides.[1−4,6]

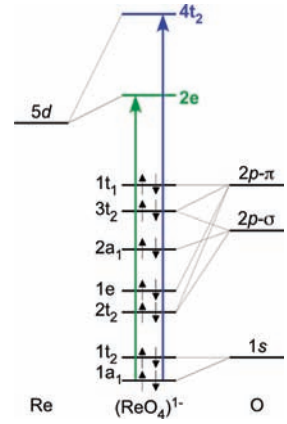

Figure 3. Qualitative molecular orbital scheme that shows an interpretation of the pre-edge transitions for $NaReO_4$.

The B3LYP DFT ground state calculations that were conducted on ReO_4^{1-} are consistent with both the molecular orbital picture determined by group theory analysis and with previous calculations reported on other MO_4^{x-} systems.[22−24,27,30,65−70] For example, the calculated electronic structure for the six highest occupied molecular orbitals of the ReO_4^{1-} anion can be described as being of t_1 and t_2 symmetries, which are essentially nonbonding and primarily consist of O 2p character, see Figure 3 and the Supporting Information. Higher in energy are unoccupied and π-antibonding orbitals of e symmetry, which are primarily of Re 5d character. These orbitals are lower in

(65) Viste, A.; Gray, H. B. *Inorg. Chem.* **1964**, *3*, 1113.
(66) Kebabcioglu, R.; Müller, Rittner, W. *J. Mol. Struct.* **1969**, *9*, 207.
(67) Müller, A.; Diemann, E. *Chem. Phys. Lett.* **1971**, *9*, 369.
(68) Rouschias, G. *Chem. Rev.* **1974**, *74*, 531.
(69) Calabrese, A.; Hayes, R. G. *Chem. Phys. Lett.* **1976**, *43*, 263.
(70) Green, J. C.; Kaltsoyannis, N.; Sze, K. H.; MacDonald, M. A. *Chem. Phys. Lett.* **1990**, *175*, 359.
(71) Green, J. C.; Guest, M. F.; Hillier, I. H.; Jarrett-Spargue, S. A.; Kaltsoyannis, N.; MacDonald, M. A.; Sze, K. H. *Inorg. Chem.* **1992**, *31*, 1588.
(72) Richter, M. M.; Brewer, K. J. *Inorg. Chem.* **1992**, *31*, 1594.
(73) Mukoyama, T.; Adachi, H. *Chem. Phys. Lett.* **1993**, *215*, 93.
(74) Bursten, B. E.; Green, J. C.; Kaltsoyannis, N. *Inorg. Chem.* **1994**, *33*, 2315.
(75) Neugebauer, J.; Baerends, E. J.; Nooijen, M. *J. Phys. Chem. A* **2005**, *109*, 1168.
(76) Xu, W.; Jianyi, M.; Peng, D.; Zou, W.; Liu, W.; Staemmler, V. *Chem. Phys.* **2009**, *356*, 219.

Table 2. The Calculated Composition for Selected Orbitals of ReO_4^{1-} [a]

	MO label (symmetry label; primary Re component)					
	25, 26 (e; 5d)	27 (a_1; 6s)	28−30 (t_2; 6p)	35−37 (t_2; 5d)	38,39 (e; 6d)	40−43 (t_2; 6d)
	(LUMO)					
energy (eV)	3.03	3.08	3.92	5.10	6.49	6.50
total % Re 5d	60.9	0.0	3.8	54.8	0.0	0.0
total % Re 6p	0.0	0.0	95.4	7.7	0.0	0.0
total % Re 6s	0.0	100.0	0.0	0.0	0.0	0.0
total % Re 6d	0.0	0.0	0.0	0.0	93.2	94.1
total % O 2p[b]	38.8	0.0	0.4	36.8	5.6[c]	6.0[c]
% O 2p per bond[c]	19.4	0.0	0.3	27.6	2.8	4.5

[a] Alpha orbital energies are reported. [b] The degree of O 2p and 3p mixing with Re 6d orbitals could not be determined from this DFT analysis, and more advanced calculations are currently underway to better evaluate the composition of these molecular orbitals. [c] % O 2p per bond values were determined by dividing the total % O p character by the number of bonding oxygen atoms multiplied by the orbital degeneracy.

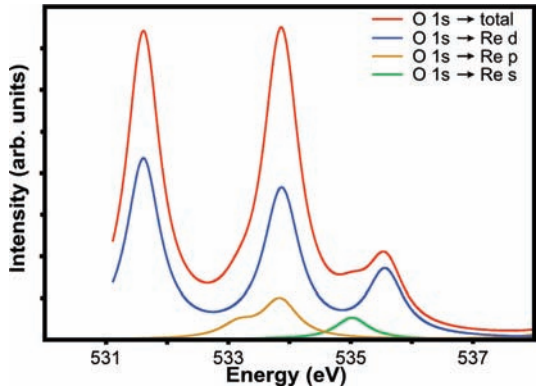

Figure 4. TD-DFT calculated ReO_4^{1-} O K-edge XAS spectrum (red) that shows contributions from the O 1s electronic excitations to molecular orbitals primarily consisting of Re d (blue), p (brown), and s (green) character.

energy by 2.07 eV (16 696 cm^{-1}) than the higher lying $\sigma + \pi$ antibonding orbitals of t_2 symmetry, which are also predominantly Re 5d. The ground-state DFT also indicate that at energies in between the Re 5d e and t_2 orbitals exist a non-bonding Re 6s orbital (a_1) and t_2 orbitals that contain primarily Re 6p character. Overall, these calculations suggest that the first two features in the $NaReO_4$ O K-edge XAS spectrum stem from O 1s electronic excitations to the molecular orbitals that result from Re 5d and O 2p mixing, and specifically involve the orbitals of e and t_2 symmetries, respectively, Figure 3.

TD-DFT Calculations. The ReO_4^{1-} O K-edge XAS experimental spectrum was simulated using time dependent-density functional theory (TD-DFT),[15,20] and Figure 4 shows contributions to the calculated spectrum from transitions associated with molecular orbitals that contain primarily Re s, p, and d character. The calculation is in excellent agreement with the experimental data, Figure 5. The simulated spectrum was shifted by a constant 13.7 eV, to account for the omission of the atomic relaxation associated with the core excitation, relativistic stabilization, and errors associated with the functional.[61] The calculated spectra predict three pre-edge features with relative peak heights and peak splittings that agree well with the experimental data. The TD-DFT calculations are consistent with group theory and ground-state DFT analysis, and the first pre-edge feature is attributed solely to an O 1s → e transition, whereas the second

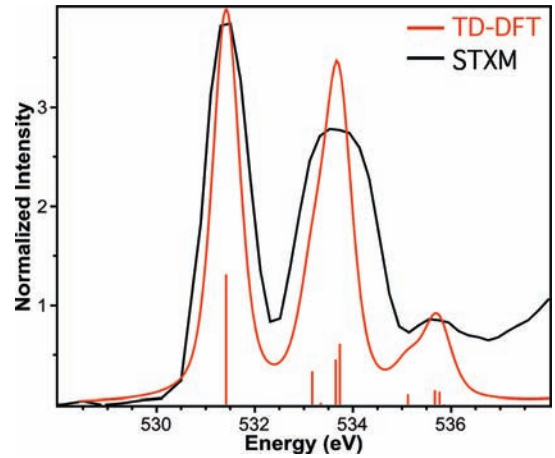

Figure 5. O K-edge X-ray absorption spectra for $NaReO_4$ obtained by scanning transmission X-ray microscopy (STXM; black), the TD-DFT calculated spectrum (red), and calculated transitions (red bars). The height of the red bars represents the calculated oscillator strength for the individual transitions.

feature is attributed primarily to an O 1s → t_2 transition. The TD-DFT calculation predicts an energy gap between the e and t_2 orbitals of 2.3 eV, which is also consistent with the observed peak splitting of 2.2(1) eV (mean value of the FY, STXM, and NRIXS results) and with general expectations for a third row transition metal with four O^{2-} ligands.[64,65] The calculations also suggest that weak unresolved transitions to higher lying molecular orbitals that consist mostly of Re 6s and 6p character are possible, which is consistent with previous photoelectron spectroscopic analysis of OsO_4.[70,71] These weak additional transitions potentially account for the significant broadening observed for the t_2 peak relative to the e feature. However, it is additionally possible that spin−orbit coupling of the t_2 (5d) level,[74] which has not been accounted for in these TD-DFT calculations, also contributes to the greater width of the absorption band assigned to this virtual orbital, as observed previously for OsO_4.[70,71] Further experimentation is underway to understand the origin of this broadening.

The comparison of experimental and simulated O K-edge XAS data for $NaReO_4$ offers a unique opportunity to evaluate the participation of the metal valence orbitals in the Re−O bond. For example, the pre-edge features in the ReO_4^{1-} spectrum result from bound state transitions that involve oxygen 1s electron excitations to primarily rhenium based molecular antibonding orbitals. Given the small spatial overlap between the O 1s and atomic Re 5d orbitals, the intensities for these transitions are best described as O 1s → 2p transitions, weighted by the amount of covalent mixing in the Re−O bond.[6] Thus, the percent O 2p character per Re−O bond can be related to the experimentally determined pre-edge intensities, which were derived from curve fits in analogy to the Cl and S covalency measurement developed by Solomon, Hedman, and Hodgson.[6] Consistently, the experimentally determined e to t_2 pre-edge peak intensity ratios are 0.72 and 0.73 for the NRIXS and STXM measurements, respectively. The intensity ratios for these features are in close agreement with the O 2p orbital mixing coefficients associated with the respective eigenvectors as demonstrated by comparison with the Mulliken analysis. These calculations show the O 2p character ratio for the e to t_2 orbitals (which consist of primarily Re 5d character) is 0.70, Table 2, and in close accord with the ratio of degeneracies (2/3=0.67). This manifold of Re 5d + O 2p orbitals in the virtual space indeed corresponds to the

antibonding combination of the actual bonding orbitals (HOMO-11 to HOMO-7) of Re 5d with O 2p, see the Supporting Information. The occupied orbitals have, on average, 40% Re 5d character and 60% O 2p, the opposite being true for the unoccupied orbitals that yield the first two peaks in the spectrum.

One curiosity associated with the experimental and simulated $NaReO_4$ O K-edge spectra is the origin of the third weak pre-edge feature (535.9 eV), which is not easily explained using simple group theory analysis. The electronic structure calculations suggest that the transition may be associated with a manifold of Re 6d Rydberg-type orbitals weakly split by the tetrahedral ligand field (see molecular orbital pictures in Supporting Information). Allowed transitions that involve these electronic states stem from small mixing, in the virtual space alone, of the Re 6d orbital in bonding and antibonding combinations with the O 2p and 3p orbitals, which is apparent in the calculations. This suggests that the third pre-edge feature is not associated with the virtual antibonding counterpart of any actual occupied bonding orbitals, and is likely not indicative of ground state bond covalency at all. Based on the calculations, it is tempting to attribute this third feature to a transition into a "bonding" combination of virtual orbitals, where the corresponding "antibonding" mix is at even higher energy and cannot be resolved from the white line. However, additional experiments are needed, and are currently underway, to validate this interpretation. It is clear from both theory and experiment that this third feature, so small in comparison to the $1s \rightarrow e$ and $1s \rightarrow t_2$ peaks, is essentially insignificant in terms of the M−O bond.

Concluding Remarks

Despite the inherent difficulties associated with obtaining accurate X-ray absorption spectra (XAS) on first row atoms, i.e., oxygen, it seems promising, based on this study, that correct O K-edge data can be obtained and used to evaluate metal-light atom ligand bonding in nonconducting molecular compounds. We find that direct comparison between NRIXS and XAS, in three different detection modes (TEY, FY, and STXM), provides a sound basis for validation of spectra that could otherwise be partially or completely incorrect. In this case, the multiple techniques and detection methods work quite cooperatively. For example, agreement between the FY, STXM, and NRIXS data allows identification of the true, bulk-like excitation spectrum. The NRIXS measurement provides a bulk-sensitive hard X-ray (~10 keV) technique that is immune from the several well-known possible sources of systematic errors for XAS measurements at low photon energies, while the XAS experiments allow definitive identification of spectral details which are difficult to observe using NRIXS. In addition, agreement between the NRIXS and STXM spectra provides confidence that quantitative pre-edge intensities can be obtained and potentially used in future studies to evaluate the amount of O 2p character in other M−O bonds.

Although additional experiments are needed to determine the generality of these results, this study suggests that $NaReO_4$ may serve as a convenient and well-defined energy and intensity standard for light atom K-edge covalency studies using XAS and NRIXS measurements. The T_d-$NaReO_4$ compound is desirable as a standard since it represents a highly symmetric d^0 compound that is air and moisture stable, commercially available, and easily purified by recrystallization. Experiments are underway to test the utility of $NaReO_4$ as a standard, which could have widespread impact given the success of similar Cl and S ligand K-edge XAS studies in terms of understanding ground state properties and advancing modern electronic structure theory for M−Cl and M−S bonding.[1−21] We are especially excited about extending O K-edge XAS and NRIXS measurements to f-element systems, where the near degeneracy of O 2p and actinide 5f and 6d orbitals is anticipated to provide significant orbital mixing.

Acknowledgment. We are grateful to Professor Jennifer C. Green for helpful discussions and to insights provided by several anonymous reviewers. This work was supported at Los Alamos by the Division of Chemical Sciences, Geosciences, and Biosciences, Office of Basic Energy Sciences, U.S. DOE, under the Heavy Element Chemistry Program at LANL, the Glenn T. Seaborg Institute postdoctoral fellowship (P.Y.), Glenn T. Seaborg Institute graduate fellowship (J.B.), and Frederick Reines postdoctoral fellowship (S.A.K.). The work at the ALS Beamline 11.0.2 and LBNL were (D.K.S., T.T.) was supported by the Director, Office of Science, Office of Basic Energy Sciences, and the Division of Chemical Sciences, Geosciences, and Biosciences of the U.S. Department of Energy at Lawrence Berkeley National Laboratory under Contract No. DE-AC02-05CH11231. Work at the University of Washington (GTS) was supported by the U.S. Department of Energy Basic Energy Sciences. Portions of this research were carried out at the Stanford Synchrotron Radiation Laboratory (SSRL), the Advanced Light Source (ALS), and the Advanced Photon Source (APS), all of which are national user facilities supported by the U.S. Department of Energy, Office of Basic Energy Sciences. Los Alamos National Laboratory is operated by Los Alamos National Security, LLC, for the National Nuclear Security Administration of U.S. Department of Energy under Contract DE-AC52-06NA25396. PNC/XOR facilities at the Advanced Photon Source, and research at these facilities, are supported by the U.S. Department of Energy−Basic Energy Sciences, a Major Resources Support grant from NSERC, the University of Washington, Simon Fraser University and the Advanced Photon Source. Use of the Advanced Photon Source is also supported by the U.S. Department of Energy, Office of Science, Office of Basic Energy Sciences, under Contract DE-AC02-06CH11357.

Supporting Information Available: For the NRIXS, FY, and STXM data, plots of energy vs normalized intensity for the $NaReO_4$ O K-edge spectra are provided that show experimental data, curve fits, residual features, and the negative amplitudes of the Gaussian functions used to generate the fits. In addition, TD-DFT calculated spectra are provided that show contributions from O 1s electronic excitations to molecular orbitals that primarily consist of Re s (green), p (blue), and d (pink) orbitals as well as an analysis of the sensitivity of the predicted spectrum to some simulation parameters such as functional, basis set, and methodology. Density of unoccupied states in a crystal simulation of $NaReO_4$ calculated with hybrid DFT and decomposed in angular momentum components are included, as well as the calculated molecular orbitals, bond lengths, charge, and orbital composition for representative occupied and unoccupied orbitals of ReO_4^{1-}. Complete refs 39, 40, and 52 are also included. This material is available free of charge via the Internet at http://pubs.acs.org.

JA1040978